https://doi.org/10.1016/j.ijhydene.2018.11.159

Plastic waste fuelled solid oxide fuel cell system for power and carbon nanotube cogeneration

Weizi Cai[a,b], Peipei Liu[a], Bin Chen[b], Haoran Xu[b], Zhijun Liu[a], Qian Zhou[a], Fangyong Yu[a,c], Meilin Liu[a,d], Meina Chen[b,e], Jiang Liu[a,*], Meng Ni[b,*]

[a] New Energy Research Institute, School of Environment and Energy, South China University of Technology, University City, Guangzhou, Guangdong 510006, P. R. China.

[b] Building Energy Research Group, Department of Building and Real Estate, The Hong Kong Polytechnic University, Hung Hom, Kowloon, Hong Kong 999077, P. R. China.

[c] School of Chemical Engineering, Shandong University of Technology, Zibo, Shandong 255049, P. R. China.

[d] School of Materials Science and Engineering, Georgia Institute of Technology, 771 Ferst Drive, Atlanta, GA 30332-0245, USA.

[e] School of Physics and Electronics, Shandong Normal University, Jinan, Shandong Province 250014, P. R. China.

Abstract

This paper reports a novel process for simultaneous power generation and green treatment of plastic waste by a solid oxide fuel cell (SOFC) integrated with pyrolysis-gasification processes. With an electrolyte-supported configuration, the

*Corresponding author:
Tel: +86 20 22236168, Fax: +86 20 22236168, E-mail: jiangliu@scut.edu.cn (Prof. Jiang LIU)
Tel: +852 27664152, Fax: +852-27645131, Email: bsmengni@polyu.edu.hk (Prof. Meng NI)

SOFC delivers a power output of 71 mW cm^{-2} at 800 °C, which is improved to 280 mW cm^{-2} after applying reforming catalyst. The microstructures and properties of the reforming catalyst before and after operation, the components of the pyrolysis products of plastic waste, and the mechanism and effect of the reforming catalyst to the SOFC are analysed and discussed in detail. In addition, carbon nanotubes are observed in the catalytic pyrolysis of plastic waste, suggesting it is also a potential technology for electricity-carbon nanotube cogeneration. This work demonstrates the feasibility of SOFCs for electricity-carbon nanotube cogeneration and green treatments of municipal solid wastes simultaneously.

Keywords: plastic wastes; solid oxide fuel cell; pyrolysis-gasification; reforming catalyst; solid wastes treatment

1. Introduction

Globally, more than 7 billion tonnes of municipal solid wastes (MSW) are produced every year. How to effectively treat the solid waste without negatively impacting the environment remains a big challenge for the society, especially for metropolis [1]. Plastic waste is one of the major parts of MSW, typically about 10 wt.% [2] and this value is even 19.5wt.% for Hong Kong according to Environment Protection Department of Hong Kong Government. Currently, the MSW including the plastic wastes are primarily treated by landfill or incineration. However, both

landfill and incineration are not effective and not environmental-friendly, due to the contamination of the soil and the underground water by landfills and the air pollution and toxic gas emission from incineration plants. In Hong Kong, the MSW especially the plastic wastes are disposed at the landfill sites which are almost full. It is thus very urgent to develop alternative and effective ways for plastic waste treatment with low impact to the environment.

Pyrolysis-gasification process is a promising way to recycle plastic wastes [3-5]. Dozens of studies have been reported on catalytic pyrolysis of plastic wastes for producing valuable products, such as gases and oils for industrial use [6-10]. In the pyrolysis-gasification process, plastic wastes are thermally decomposed into gases, oils and tars under high temperature and hypoxic atmosphere. The component and amount of the pyrolysis products can be significantly changed by varying the operational conditions. For example, hydrogen production could be greatly increased while the oils and solid production could be reduced by using suitable reforming catalysts for the pyrolysis-gasification process [11, 12]. As the major gas product of the pyrolysis-gasification process, hydrogen is regarded as an ideal fuel for fuel cells with environment-friendliness and high energy efficiency [8]. Solid oxide fuel cells (SOFCs) with solid state electrolyte are energy conversion devices that can directly convert the chemical energy of fuel into electricity with high efficiency [13]. More importantly, the high reactivity of O^{2-} which transports through the electrolyte from the cathode side to the fuel electrode side allows an SOFC to be operated on any combustible fuel, such as hydrogen, carbon monoxide[14, 15], carbon [16-20],

methane [21-23], gasoline [24-26], and even biomass-derived fuel [27-30]. Almond shell biochar and coconut biochar are utilized to generate electricity in SOFCs by Elleuch et. al. and relatively high performances of 127 mW cm^{-2} and 105 mW cm^{-2} at 700 °C are achieved respectively [31]. A direct octane fuel cell system using transportation fuel (iso-octane) without co-feeding of O_2 and CO_2 is developed by Liu's group, which demonstrates a maximum power density of about 0.6 W cm^{-2} at 750 °C [32]. With high energy density (6.260 kWh L^{-1} and 5.442 kWh L^{-1}), bioethanol and glycerol are directly used as fuel in a low-temperature SOFC system by Qin et.al. [27]. Using glycerol, a peak power density of 215 mW cm^{-2} at 580 °C is achieved. Medium density fibreboard, as waste-derived carbon, is also chosen as carbon fuel to power a hybrid direct carbon fuel cell by Jiang et.al. [33] and offer a realistic alternative technology for clean utilization of solid waste. The above-mentioned studies, clearly demonstrate that SOFC is a promising technology for energy conversion from solid waste.

In this study, a novel process is proposed to directly treat plastic waste for clean power generation by SOFCs, involving a two-stage pyrolysis-gasification reaction process. The disposable plastic lunch box mainly composed of polypropylene is chosen in this study, since polypropylene is a major component of general plastic wastes. To further enhance the SOFC performance, catalyst for the pyrolysis-gasification of plastic waste is used. For comparison, the performance of H_2-fuelled SOFC is also measured. The microstructures and crystal structure of the catalyst, pyrolysis properties of the plastic wastes and the output performance,

impedance spectra, and discharging characteristics of the corresponding SOFCs are examined and analysed in detail.

2. Experiment

2.1 Fabrication of SOFCs

Button cells with a configuration of Ag-GDC/ YSZ/ Ag-GDC were fabricated. Firstly, an electrolyte support of yttria-stabilized zirconia (8YSZ, Tosoh Corporation, Japan) was fabricated by dry pressing method (0.18 g in weight and 13 mm in diameter), followed by sintering at 1400 °C in air for 4 h [34]. A dense YSZ electrolyte wafer with a thickness of 0.3 mm and a diameter of 11 mm was obtained. Secondly, silver paste (DAD-87, with 70 wt.% Ag, Shanghai Research Institute of Synthetic Resins, Shanghai, China) and GDC powder (purity $\geqslant$ 99.5 % , particle size: d50= 0.5~3 um, Ningbo Institute of Materials Technology and Engineering, China) were ground in an agate mortar for 3 h to get an uniform Ag-GDC slurry (weight ratio of 70:30). Then the slurry was painted on both sides of the electrolyte pellets followed by firing at 850 °C for 4 hours. The cathode area was controlled to be 0.32 cm^2. Thirdly, the silver paste was painted in reticular shape, as current collector, on the surface of electrodes.

2.2 Preparation of reforming catalyst

Ni-Al-Mg catalysts were prepared by co-precipitation method. Ammonia

solution (25 wt. %, Guangzhou Chemical Reagent Factory, China) was added to a mixed aqueous solution of $Ni(OH)_2 \cdot 6H_2O$, $Mg(NO_3)_2 \cdot 6H_2O$ and $Al(NO_3)_3 \cdot 9H_2O$ (with a mol ratio of Ni: Al: Mg as 1:1:1, A.R., Guangzhou Chemical Reagent Factory, China) drop by drop under stirring until the pH reaches about 8. Then, the precipitates were filtered and washed with deionized water, followed by drying at 110 °C for 12 h. Finally, the dried precursors were calcined in air at 750 °C for 4 h to obtain the Ni-Al-Mg powders. The crystal phase structure of Ni-Al-Mg before and after operation were measured by an X-ray diffraction (XRD, Rigaku D/max-IIIA diffractometer, Japan, Cu-Ka radiation, operated at 35 kV, 30 mA, l = 1.5406 Å).

2.3 Characterization of the pyrolysis products of plastic wastes

TG and DTA measurements were carried out using a thermogravimetric analyzer (Mettler Teledo TGA/DSC 1, Switzerland) to determine the pyrolytic properties of the plastic waste. It was heated from room temperature to 1000 °C at 10 °C min^{-1} in pure N_2 atmosphere.

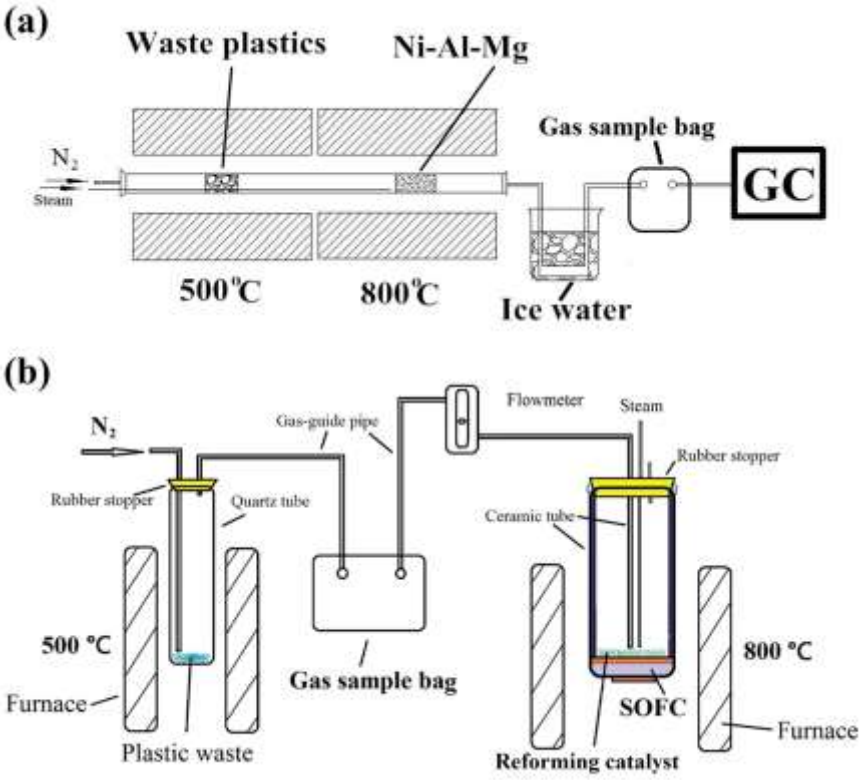

Fig. 1 – The measurement system for the pyrolysis products of plastic wastes (a) and schematic diagram of the SOFC system fuelled by plastic wastes (b).

The pyrolysis products of plastic wastes with and without reforming catalyst (Ni-Al-Mg) were measured through a pyrolysis-gasification system as shown in Fig. 1(a). A disposable plastic lunch box (Polypropylene, food grade, Yuge plastic products factory, Fujian, China) was cut into strips (5 mm × 20 mm). The plastic waste (1.0 g) was placed in the left side of a long quartz tube whose temperature was kept at 500 °C. The gas products generated from the plastic wastes passed through the reforming catalyst, where the pyrolysis temperature was 800 °C. After catalytic pyrolysis at the right reactor, the hot gas products were cooled through an ice water bath before entering a Gas Chromatography system (Agilent Technologies 7890B,

USA). The right furnace was first heated to 800 °C, before the left furnace was heated to 500 °C at a heating rate of 30 °C min^{-1}. Nitrogen is used as carrier gas with a flow rate of 50 mL min^{-1} during the entire catalytic pyrolysis process. Carbon nanotubes generated by the plastic wastes are collected by the following steps. Firstly, the catalysts and carbon nanotubes mixtures are immersed in dilute hydrochloric acid under stirring. After being stirred for ten hours, catalysts can be totally dissolved in dilute hydrochloric acid, while carbon nanotubes still remain solid state. Secondly, the suspensions are filtered and washed several times using pure water, until the pH value of the filtrate reaches 6~7. Thirdly, the carbon nanotubes are collected and heated in an oven at 100 ºC, until the carbon nanotubes are completely dry. Finally, the dry carbon nanotubes are weighed.

2.4 Cell assembling and characterization

Silver paste was used as sealing and jointing materials to connect each of a single cell to one end of a corundum ceramic tube. Some of the cells were firstly tested with hydrogen fuel in the way reported previously [35]. The flow rate of hydrogen was 30 mL min^{-1}. Fig. 1(b) shows the schematic diagram of an SOFC system fuelled by plastic waste. A quartz tube with an opening end was set inside the left furnace, while a corundum ceramic tube with an SOFC sealed on one end was set inside the right furnace. A gas sample bag was applied to connect the plastic waste part (quartz tube) and the SOFC part (corundum tube). Plastic waste strips (10.0 g) were placed in the quartz tube heated by the left furnace, so that the pyrolysis

temperature of 500 °C could be accurately controlled. Reforming catalyst (Ni-Al-Mg) was filled into the corundum tube and tiled on the cell. The SOFC part was first heated to operation temperature, before the plastic waste part was heated to 500 °C at a heating rate of 30 °C min^{-1}. The primary pyrolysis gas products of plastic waste were first stored in the gas sample bag, then supplied to reforming catalyst bed within the SOFC part with a flow rate of 50 mL min^{-1}. At the same time, steam was also introduced into the reforming catalyst bed with a flow rate of 75 mL min^{-1}. The other ends of the corundum ceramic tube and the quartz tube were blocked by a rubber stopper along with a plastic gas-guide pipe for leading the emitted gas out and sealed up by some petrolatum jelly and Teflon tapes.

Three cells filled with different fuel were tested and characterized (Cell-1, with humidified hydrogen as fuel; Cell-2, with plastic waste as fuel and without catalyst; Cell-3, with reforming catalyst and plastic wastes as fuel). Ambient air was the oxidant for all these three SOFCs. The electrochemical performances of these cells were characterized by an Iviumstat electrochemical analyzer (Ivium Technologies B.V., Netherlands). The electrochemical impedance spectroscopies (EIS) of the cells were measured at open circuit voltage (OCV) at 800 °C with a frequency range from 0.1 Hz to 10 KHz. The microstructures of the cells and the reforming catalyst were characterized using a scanning electron microscope (SEM, Philips XL-30FEG, Holland and Carl Zeiss AG-Merlin, Germany) equipped with energy-dispersive X-ray (EDX).

3 Results and discussion

3.1 SEM pictures of the as-prepared SOFCs

The microstructures of the cross-section (a) and the anode (b) of the as-prepared SOFCs are illustrated in Fig. 2. A quite dense and thick electrolyte of about 300 μm can be observed in Fig. 2(a). The 20 μm thick anode is uniform in morphology and highly porous, suggesting sufficient reactive sites. It closely attaches to the YSZ electrolyte substrate, as shown in Fig. 2(b).

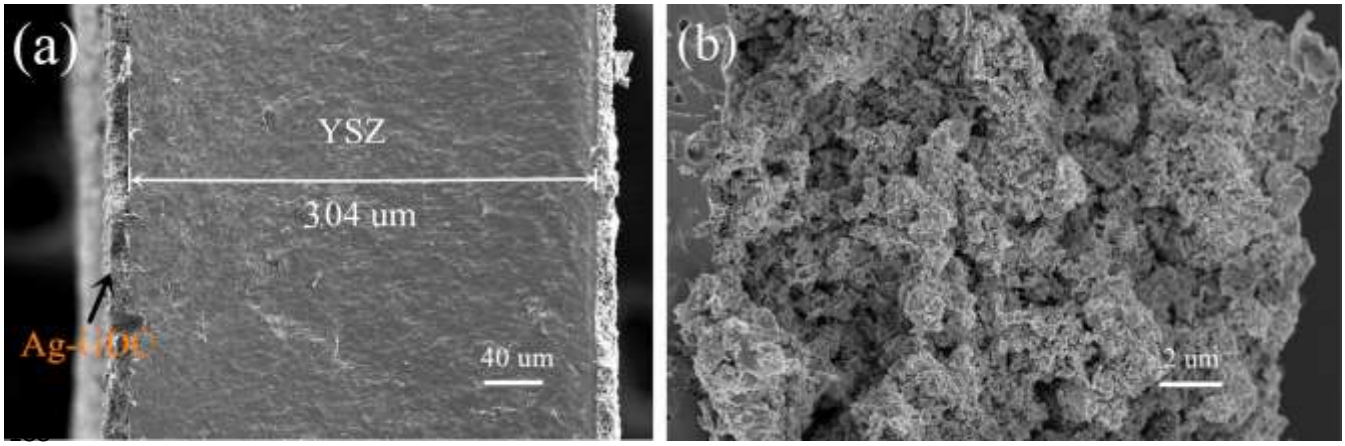

Fig. 2 – The microstructure of cross-section (a) and anode (b) of the as-prepared SOFC.

198 *3.2 Properties of the plastic waste and reforming catalyst (Ni-Al-Mg)*

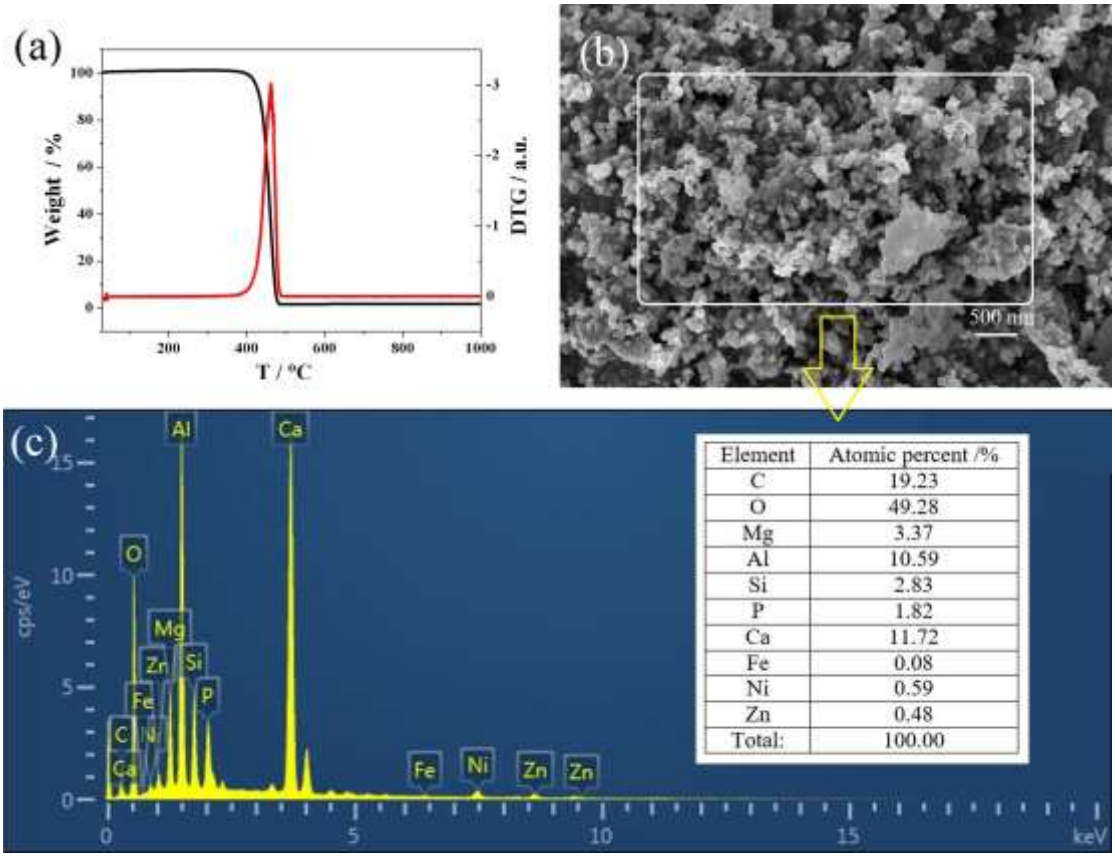

Element	Atomic percent /%
C	19.23
O	49.28
Mg	3.37
Al	10.59
Si	2.83
P	1.82
Ca	11.72
Fe	0.08
Ni	0.59
Zn	0.48
Total:	100.00

199

200 **Fig. 3 – TG curves (a) of the plastic wastes in N_2 atmosphere, SEM picture (b)**

201 **and EDX spectra (c) of the inorganic remainders of the plastic wastes after TG**

202 **measurement.**

203

204 The TG and DTG curves of the plastic wastes in N_2 atmosphere, along with an

205 inset of locally enlarged view, are presented in Fig. 3(a). Obviously, a major weight

206 loss of the plastic waste at about 450 °C can be observed from the TG curve, which is

207 attributed to the pyrolysis of polypropylene contained in the plastic waste. It can be

208 seen from the DTG curve, the pyrolysis rate of polypropylene rapidly speeds up at

209 400 °C and reaches a maximum rate at 461 °C. Above 480 °C, the polypropylene in

plastic wastes is completely decomposed into gases. After thermogravimetric measurement, only 1.7 wt. % of solid inorganic substances remain, which are some inorganic additives of the plastic. The inorganic additives are added into the plastic products to improve the mechanical strength and processability of the plastic products, as well as reduce cost of raw materials. In the experiment, plastic waste is placed in the first reactor, so the inorganic additives would not affect the cell. To further study the composition of plastic waste, the remainders of the plastic waste after high temperature operation are characterized using SEM and EDX measurement. As shown in Fig. 3(b) and (c), the inorganic remainders are agglomerated after high temperature operation, and mainly compose of the oxides or carbonates of Ca, Mg, Al, and Si. Small amounts of Ni, Zn, Fe and P are also found from the EDX spectra (Fig. 3(c)). In real life, real plastic wastes may contain or adhere to other solid or liquid wastes. However, not all the solid or liquid wastes must be dealt with before application to the SOFC. As we have mentioned before, the plastic wastes are set in the first quartz tube, therefore solid wastes will stay in the first quartz tube and won't affect the SOFC. For the liquid wastes, the negative effect of the gasification products to the cell should be carefully considered. If the gasification products contain some poisonous materials to the cell, then the liquid wastes should be removed before application to the system.

Table 1 – Pyrolysis gaseous products composition of plastic wastes with and without catalyst (Ni-Al-Mg) at the gasification temperature of 800 °C.

	H_2	CO	CO_2	CH_4	C_2-C_4
With Ni-Al-Mg (vol. %)	58	29	5	7	1
Without Ni-Al-Mg (vol. %)	33	0	0	23	44

Table 1 shows the gas compositions of pyrolysis gaseous products of plastic waste with and without Ni-Al-Mg catalyst at the gasification temperature of 800 °C. As we can see, 33 vol. % of H_2, 23 vol. % of CH_4 and 44 vol. % of C_2-C_4 (ethane, propane, butane, ethylene, propylene and butene) are obtained from the plastic waste pyrolysis without Ni-Al-Mg catalyst. After the addition of Ni-Al-Mg catalyst, the proportion of H_2 and CO significantly increases, while that of carbon-containing organic compounds decreases, which is consistent with the results of Wu [36]. It is obvious that Ni-Al-Mg catalyst can effectively decompose alkane and alkenes with 2 to 4 carbon atoms into small molecule compounds (H_2, CO and CO_2). Moreover, the total gases yield is dramatically enhanced with the use of reforming catalyst from 47.8 % to 90.2 %, meanwhile that of oil and solid products decreases (Table 2) [36]. It is suggested that thermal cracking of large molecular products of the plastic waste is affected by the introduction of reforming catalyst and steam. It is well known that

transition metal is a highly active catalyst for catalytic pyrolysis of carbon-containing fuels. Actually, the catalytic pyrolysis process of carbon-containing fuels could be considered as a carbon deposition process of carbon-containing fuels on transition metal, which has been studied by many researches [37-39]. Generally, the carbon deposition behaviour of carbon-containing fuels on transition metal could be described as the following model [37-39]: Firstly, carbon-containing molecules are adsorbed onto the transition metal particle surface. Then, carbon atoms of the carbon-containing molecules are liberated under the catalytic effect of transition metal particle. The liberated carbon atoms dissolve and diffuse into the bulk transition metal particle from a supersaturated catalyst surface, followed by a precipitation on the other side of the catalyst particle in the form of different carbon allotropes under different conditions. Finally, the carbon deposition may cease if the catalyst particle surface is contaminated or the carbon supply is insufficient [38]. In addition, the composition of pyrolysis gases do not change with time. Because the main influence factor for the pyrolysis of plastic wastes is temperature. The higher temperature, the larger proportion of the small molecule gases (H_2, CH_4). Conversely, the lower temperature, the larger proportion of the large molecule gases (propane, propylene et. al.). In our experiment, steam is introduced into the system to achieve a higher gas yield and lower solid carbon yield, because solid carbon is hard to participate the electrochemical reaction on the SOFC anode directly. Water will significantly depress the carbon deposition, and produce more carbon monoxide and hydrogen (water gas shift reaction), which increases the total gas amount, as shown in Table 2.

Table 2 – Pyrolysis products of plastic waste (1.0 g) with catalyst weight of 0.5 g at 800 °C.

	Condition 1	Condition 2
Steam/ g	0	4.5
Catalyst	-	Ni-Al-Mg
Gas/ (plastic waste + water) (wt. %)	47.8	90.2
Solid/ (plastic waste + water) (wt. %)	30.3	5.7
Oil/ (plastic waste + water) (wt. %)	10.3	0
Mass balance (wt. %)	88.4	95.9

3.3 Cell performances

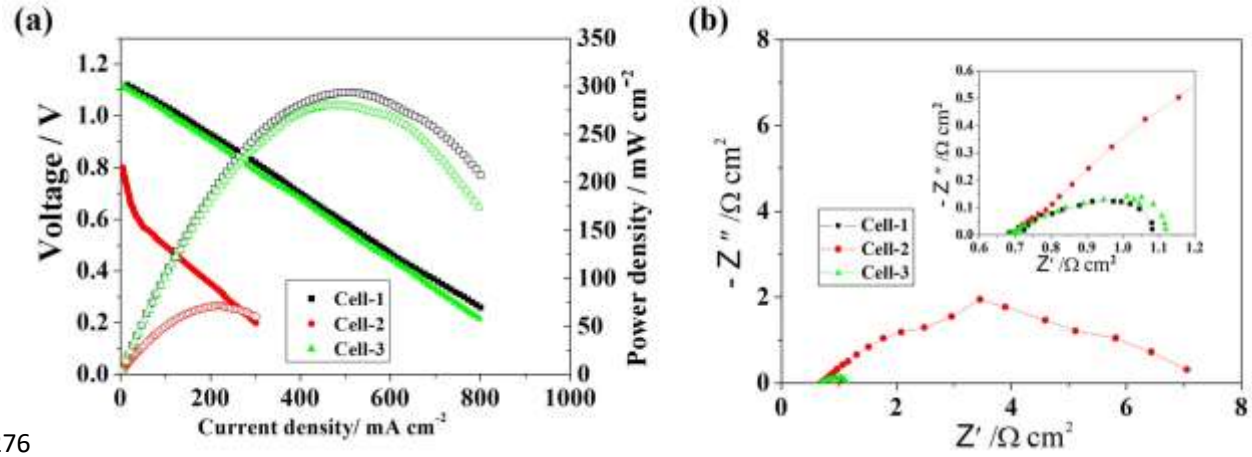

Fig. 4 – The output performances (a) and impedance spectra (b) of three different cells (Cell-1, H_2 as fuel; Cell-2, plastic wastes as fuel; Cell-3, plastic wastes as fuel and with reforming catalyst) at 800 °C. Inset is a locally enlarged one.

Table 3 – The electrochemical performances of the three SOFCs respectively operated with hydrogen, plastic wastes with and without reforming catalyst, at 800 °C.

	Cell-1	Cell-2	Cell-3
Conditions	H_2	Plastic wastes	Plastic wastes with reforming catalyst
OCV at 800 °C/V	1.12	0.80	1.12
MPD at 800 °C/ mW cm^{-2}	293	71	280
Discharging current at 0.7 V/mA	-	6	122
Discharging time / h	-	4.0	14.8

To study the feasibility of an SOFC system directly fuelled by real plastic waste, the power output and impedance spectra of the SOFC system are measured. Fig. 4 shows the output performances and impedance spectra of the three SOFCs (Cell-1, with hydrogen as fuel; Cell-2, with plastic wastes as fuel; Cell-3, with plastic wastes as fuel and Ni-Al-Mg as reforming catalyst) at 800 °C. Their OCVs and maximum power densities (MPD) are listed in Table 3. The performance of an SOFC fuelled with humidified hydrogen is measured for comparison. As we can see, the open circuit voltages of Cell-1 and Cell-3 are as high as 1.12 V, while that of Cell-2 is 0.80 V. The OCV of a SOFC is closely related to the fuel composition. We measured

the composition of the pyrolysis gases produced with and without catalyst and reforming by GC, and the results are shown in Table 1 and the Supplemental Material. As can be seen, the pyrolysis gas produced without the reforming catalyst and steam contains large amount of high-carbon (C_2, C_3, and C_4) molecules which are not as active as those smaller molecules (H_2, CO, CH_4) constituting the reformed gas. This can explain the low OCV of Cell-2 using the former gas as the fuel. The peak power density of Cell-1 with humidified hydrogen fuel is 293 mW cm^{-2}. It is reasonable for an electrolyte-supported SOFC (thickness: 300 μm), whose resistance was dominated by ohmic resistance of the electrolyte. For the cells operated on plastic wastes (Cell-2 and Cell-3), reforming catalyst significantly promotes the output performance of SOFC, from 71 mW cm^{-2} (Cell-2) to 280 mW cm^{-2} (Cell-3). Fig. 4(b) shows the impedance spectra of the SOFCs (Cell-1, Cell-2, and Cell-3) operated at 800 °C under OCV. As can be seen from the intercept of the real axis at high frequency from the impedance spectra, the ohmic resistances of all the cells are identical, 0.69 Ω cm^2. Due to the limited accuracy of the testing instrument and lowest applied frequency, 0.1 Hz, only one quadrant of the Nyquist plot can be observed and there is no low-frequency intercept with the real axis. As expected, the variation trend of polarization resistance of the cells is consistent with that of the I-V-P curves. The polarization resistances of the hydrogen SOFC (Cell-1, 1.08-0.69=0.39 Ω cm^2) is slightly smaller than that of the plastic waste SOFC with reforming catalyst (Cell-3, 1.11-0.69=0.42 Ω cm^2), and obviously smaller than that of the cell operated on plastic wastes without reforming catalyst (Cell-2, 7.05-0.69=6.36 Ω cm^2). It can be presumed

that the difference of polarization resistances of Cell-2 and Cell-3 is caused by the catalysis of Ni-Al-Mg. At 500 °C, polypropylene would decompose into hydrocarbons with two to four carbon molecules, such as ethane, ethylene, propene and butylene, which would directly participate in the electrochemical reaction in SOFC if no reforming catalyst is used. As these hydrocarbons are less active and heavier than H_2, the performance of SOFC is poor. However, with reforming catalyst, the hydrocarbons would further decompose into H_2, CO and a small amount of solid carbon on reforming catalyst. It means that H_2 and CO instead of heavier hydrocarbon fuels will participate in the electrochemical reactions, which can significantly reduce the polarization resistance and improve the SOFC output performance. In addition, the coking problem of heavier hydrocarbon fuels is a nonnegligible issue for an SOFC, especially for a Ni anode-supported SOFC. Nevertheless, with the reforming catalyst, it can be effectively solved, and leads to an improved lifetime of the plastic waste-fuelled SOFC.

Fig. 5(a) shows the discharging curves of the two SOFCs with and without reforming catalyst at 800 °C. The cells were operated at fixed currents of 122 mA and 6 mA, respectively. As we can see, the discharging curve of Cell-2, without reforming catalyst, is quite unstable, especially at the later stage. After struggling to discharge for about 4 hours, Cell-2 finally declines. As we all know, alkanes, including methane, ethane and propane, may be problematic for a Ni anode-supported SOFC since they can lead to serious carbon deposition and thus reduce the cell performance. Large amount of alkenes gases could be lethal for an SOFC, which explains the short

and unstable discharging curve of Cell-2. However, with reforming catalyst, Cell-3 can be continuously discharged with a smooth platform of about 0.7 V at a 20 times higher current (122 mA) for about 15 h. Although there is still 1 % of alkanes in the gas products of plastic waste in the presence of reforming catalyst, it does not affect the performance and lifetime of the SOFC, which could be attributed to the excellent resistance to carbon deposition of anode materials (Ag-GDC) [17, 35]. The discharging platform of Cell-3 is quite stable, and lasts for about 10.5 h, followed by a slow recession for another 4.3 h. The amount of power generation is 6048 C, as the cell discharges for 15 h at a current of 112 mA. Therefore, for 10 g of plastic waste, the specific power generation is 604.8 C/g. The reason for the recession of the cell is due to the supply of the fuels gases, because the cell could continue to discharge after supplement of plastic waste. Unlike conventional SOFCs supplied on external gas sources, the operation time of this kind of SOFC system is limited by the amount of the fuel preloaded in the system before operation. From this specific perspective, it is similar to the direct carbon solid oxide fuel cells, whose operation time is also hindered by the consumption of carbon fuel and deactivation of Boudouard reaction catalyst. Actually, the DC-SOFC system can be improved and realize a continuous fuel feed and long-term discharging operation, which is reported by Lü et. al. [40]. By the same token, this SOFC system fuelled by plastic waste can provide a long-term discharging time through optimization of the system design. Although a discharging test of 15 h is not a sufficient evidence for the advantages of this SOFC system, it demonstrates the feasibility of plastic waste fuelled SOFC system and lays the

foundation for future improvement.

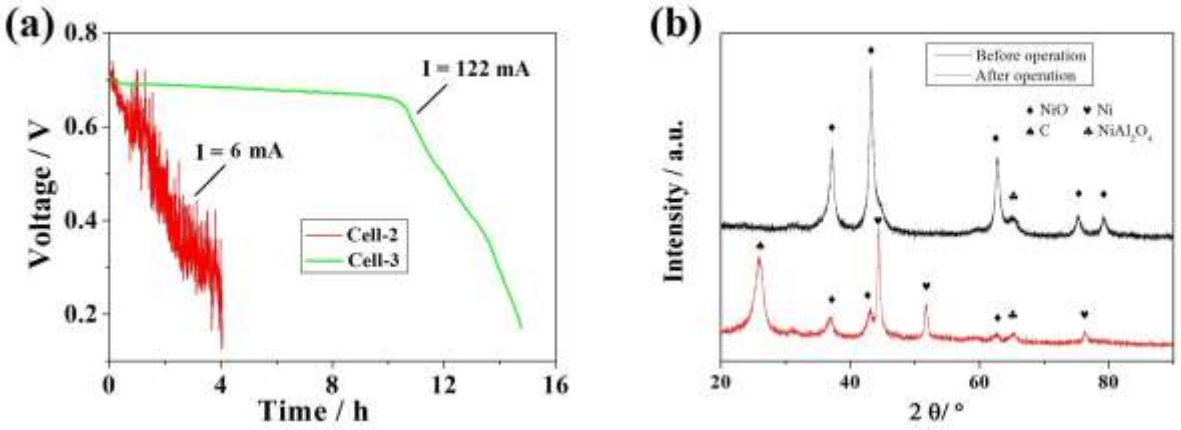

Fig. 5 – The discharging curves (a) of the two SOFCs (Cell-2 and Cell-3) and XRD (b) of the reforming catalyst before and after operation.

3.3 Characterization of the reforming catalyst before and after discharging test

To characterize the detailed structure and composition of the reforming catalyst before and after discharging test, X-ray analysis, SEM and EDX were performed, as presented in Fig. 5(b), Fig. 6 (a) and (b). As can be seen from the diffraction pattern (Fig. 5b), the main phase of the Ni-Al-Mg catalyst before discharging test is face-centered cubic (FCC) structure of NiO. In addition, the weak diffraction peak at about 65˚ might be attributed to $NiAl_2O_4$. However, after the discharging test, several obvious peaks attributed to Ni metal appear, and the peaks attributed to NiO become weak. It suggests that a majority of NiO is reduced into Ni metal after the discharging test. Moreover, there is a strong peak belonging to carbon at 25˚, implying the carbon deposition on the reforming catalyst. Fig. 6(a) and (b)

reveal the morphologies and compositions of the Ni-Al-Mg catalyst before and after discharging test. As can be seen from Fig. 6(a), the particle size of catalyst before discharging test is about 20 μm with a considerable rough surface. Interestingly, after discharging test, lots of carbon nanotubes are found on the reforming catalyst, as shown in Fig. 6(b). The EDX results of the reforming catalyst before and after discharging test show that carbon atomic percent increases significantly from 16.66 % to 77.57 %, which demonstrates the existence of carbon nanotubes. As has been mentioned above, different operation conditions result in different carbon allotrope. Only when the dissociation, diffusion and segregation of carbon atoms reach a balance, would the carbon nanotube grow. In our experiment, Ni in the reforming catalyst plays a dominant role on the growth of carbon nanotube, because of the strong carbon-nickel interaction and high solubility of carbon in nickel. It is well known that carbon nanotube is an allotrope of carbon with a cylindrical nanostructure with many unusual properties, which are valuable for electronics, optics, mechanics and other fields of materials science and technology. The carbon nanotubes are collected after removing reforming catalysts. The amount of carbon nanotubes is 346 mg. Therefore, for 10 g of plastic waste, the specific carbon nanotube generation is 34.6 mg/g. Although many techniques have been developed to produce carbon nanotube with high quality and large-scale industrial production, catalytic pyrolysis from plastic waste may provide a practical scheme of carbon nanotube production with low cost and high efficiency.

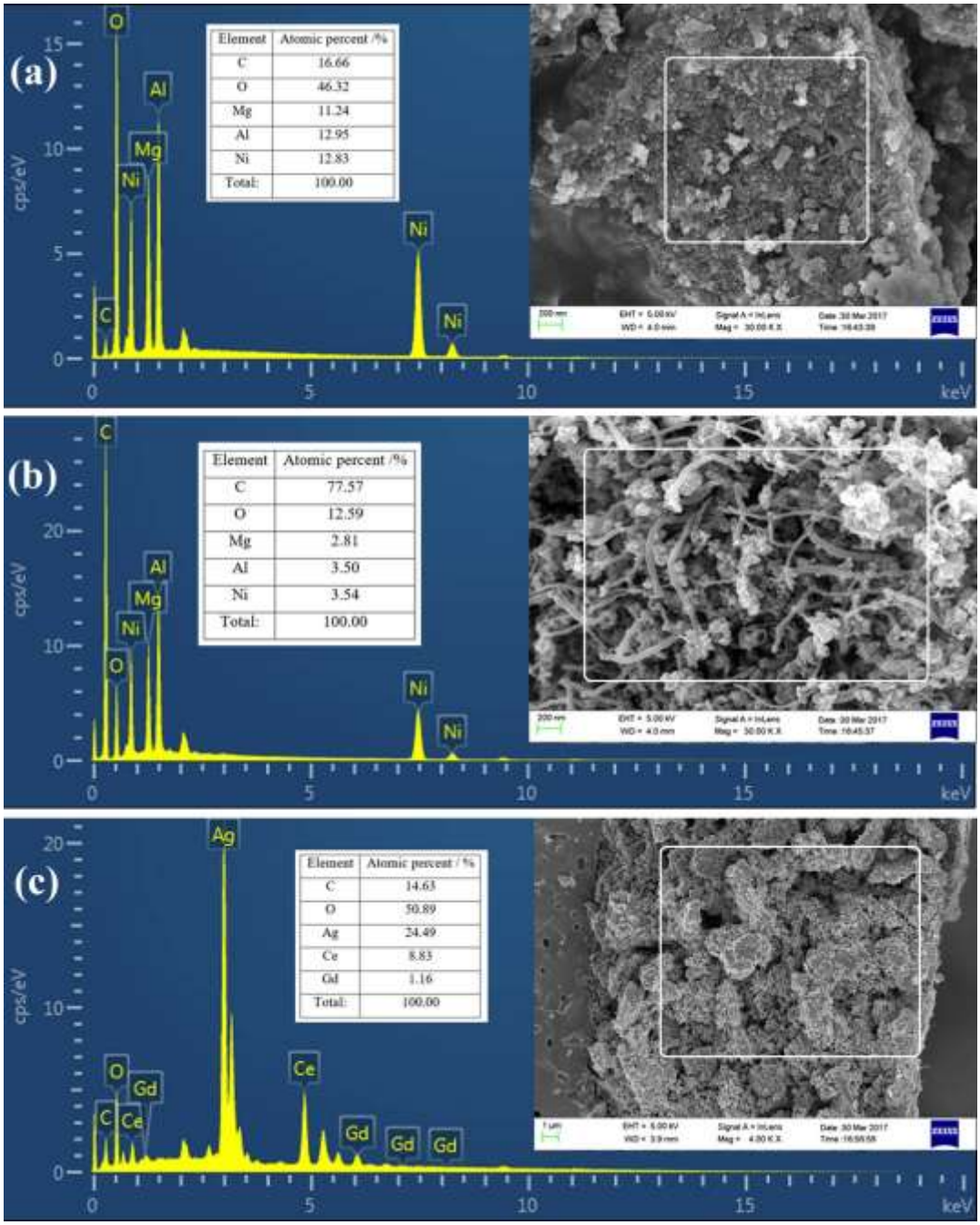

Fig. 6 – SEM pictures and EDX spectra of the reforming catalyst before (a) and after (b) operation, and the anode (c) of the cell after operation.

Fig. 6(c) is an SEM picture and EDX of the SOFC anode after discharging test. With the reforming catalyst, the microstructures of the SOFC anode after discharging test do not change so much, comparing to that before discharging test

406 (Fig. 2b). Actually, silver-GDC are excellent anode materials with high resistance of
407 carbon deposition. In our lab, an SOFC with silver-GDC as anode materials powered
408 by propane could discharge stably for over 160 h [41]. Different from an SOFC with
409 Ni anode, carbon derived from the alkanes hardly dissolve in the silver, but form an
410 amorphous covering layer, with dispersed breakages, on the surface of silver-GDC
411 anode. Although, this covering layer hindered the gaseous species diffusion,
412 hydrogen still could pass through the covering layer and keep the good stability of
413 the cell with silver-GDC anode. In this work, a small range of agglomeration and a
414 small amount of carbon could be observed in the Fig. 6(c), however it would not
415 affect the SOFC performance. The EDX spectrum of the anode shows the atomic
416 percent of carbon element is about 14.6 %, indicating that carbon deposition does
417 happen on the anode but not serious. A conclusion can be drawn that the decline of
418 the cell is not caused by the deactivation of anode material, but the insufficient
419 supply of fuels.

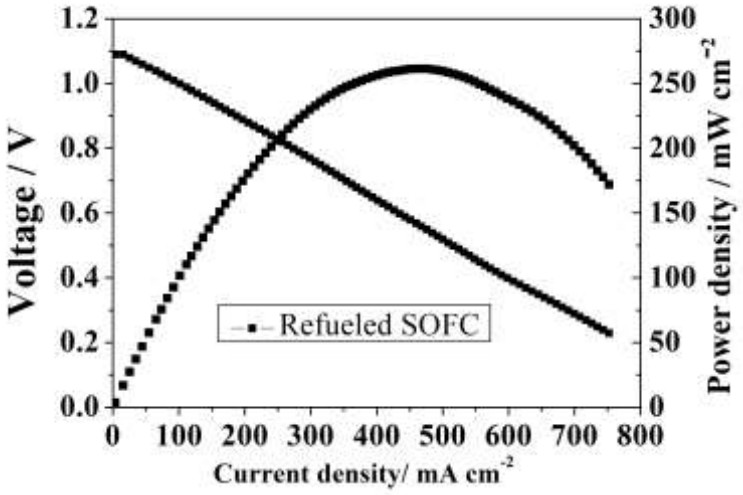

420

421 **Fig. 7 – Output performance of the refuelled SOFC (Cell-3) at 800 °C.**

422

To further demonstrate this conclusion, we refuelled the cell after the left furnace was cooled down to room temperature, heated up the left furnace to the same temperature, and retested the output performance of the cell again. As shown in Fig. 7, after a discharging test of 15 h, the SOFC still provides a OCV of 1.08 V and a peak power density of 261 mW cm^{-2} at 800 ºC, respectively, when more plastic waste is supplied to the system. Comparing to the first test (1.12 V, 280 mW cm^{-2}), the minor attenuation of the output performance is acceptable, and directly supports our conclusion.

4. Conclusions

A plastic wastes fuelled SOFC system with reforming catalyst was proposed and evaluated. With Ni-Al-Mg reforming catalyst, a maximum power density of 280 mW cm^{-2} was achieved using plastic wastes as fuel at 800 °C, which was only slightly lower than 293 mW cm^{-2} for a hydrogen SOFC and significantly higher than 71 mW cm^{-2} for a plastic wastes SOFC without reforming catalyst. Moreover, with reforming catalyst, the discharging time of the cell operated at a fixed discharging current of 122 mA, increases from 4.0 h to 15 h. It is found that reforming catalyst efficiently converts large molecule hydrocarbons and water into hydrogen and carbon monoxide, and further improve the output performance and discharging time of the SOFC. What's more, the decline of the discharging time can be attributed to the depletion of the plastic waste. In addition, carbon nanotube is found on the reforming catalyst, suggesting a potential technique for electricity and carbon nanotube cogeneration. In

conclusion, the feasibility of a plastic waste SOFC system was demonstrated which provides a novel direction for SOFCs' practical application and the management of solid waste.

Acknowledgement

This work was supported by the National Science Foundation of China (NSFC, No.91745203, U1601207, No.51602183), Program of Excellent Ph. D Thesis Authors of Guangdong Province, the Special Funds of Guangdong Province Public Research and Ability Construction (No. 2014A010106008), Guangdong Innovative and Entrepreneurial Research Team Program (No. 2014ZT05N200), The Hong Kong Polytechnic University (G-YBJN and G-YW2D), Environmental Conservation Fund of Hong Kong SAR (ECF 54/2015), RISUD (1-ZVEA).

References

[1] Ripa M, Fiorentino G, Giani H, Clausen A, Ulgiati S. Refuse recovered biomass fuel from municipal solid waste. A life cycle assessment. Appl Energy 2017; 186: 211-25.

[2] Zhou H, Meng A, Long Y, Li Q, Zhang Y. An overview of characteristics of municipal solid waste fuel in China: Physical, chemical composition and heating value. Renew Sust Energy Rev 2014; 36: 107-22.

[3] Wu C, Williams PT. Hydrogen production by steam gasification of polypropylene with various nickel catalysts. Appl Catal B: Environ 2009; 87: 152-61.

[4] Al-Rahbi AS, Williams PT. Hydrogen-rich syngas production and tar removal from biomass gasification using sacrificial tyre pyrolysis char. Appl Energy 2017; 190: 501-9.

[5] Nizami AS, Shahzad K, Rehan M, Ouda OKM, Khan MZ, Ismail IMI, et al. Developing waste biorefinery in Makkah: A way forward to convert urban waste into renewable energy. Appl Energy 2017; 186: 189-96.

[6] Aguado R, Elordi G, Arrizabalaga A, Artetxe M, Bilbao J, Olazar M. Principal component analysis for kinetic scheme proposal in the thermal pyrolysis of waste HDPE plastics. Chem Eng J 2014; 254: 357-64.

[7] Kodera Y, Ishihara Y, Kuroki T. Novel Process for Recycling Waste Plastics To Fuel Gas Using a Moving-Bed Reactor. Energy Fuel 2006; 20: 155-8.

[8] Czernik S, French RJ. Production of hydrogen from plastics by pyrolysis and catalytic steam reform. Energy Fuel 2006; 20: 754-8.

[9] He M, Xiao B, Hu Z, Liu S, Guo X, Luo S. Syngas production from catalytic gasification of waste polyethylene: Influence of temperature on gas yield and composition. Int J Hydrogen Energy 2009; 34: 1342-8.

[10] Wang N, Chen D, Arena U, He P. Hot char-catalytic reforming of volatiles from MSW pyrolysis. Appl Energy 2017; 191: 111-24.

[11] Garcia L, Benedicto A, Romeo E, Salvador M, Arauzo J, Bilbao R. Hydrogen production by steam gasification of biomass using Ni-Al coprecipitated catalysts promoted with magnesium. Energy Fuel 2002; 16: 1222-30.

[12] Acomb JC, Wu C, Williams PT. Control of steam input to the pyrolysis-gasification of waste plastics for improved production of hydrogen or

carbon nanotubes. Appl Catal B: Environ 2014; 147: 571-84.

[13] McIntosh S, Gorte RJ. Direct hydrocarbon solid oxide fuel cells. Chem Rev 2004; 104: 4845-66.

[14] Homel M, Gür TM, Koh JH, Virkar AV. Carbon monoxide-fueled solid oxide fuel cell. J Power Sources 2010; 195: 6367-72.

[15] Zhang H, Chen J, Zhang J. Performance analysis and parametric study of a solid oxide fuel cell fueled by carbon monoxide. Int J Hydrogen Energy 2013; 38: 16354-64.

[16] Cai W, Zhou Q, Xie Y, Liu J, Long G, Cheng S, et al. A direct carbon solid oxide fuel cell operated on a plant derived biofuel with natural catalyst. Appl Energy 2016; 179: 1232-41.

[17] Tang Y, Liu J. Effect of anode and Boudouard reaction catalysts on the performance of direct carbon solid oxide fuel cells. Int J Hydrogen Energy 2010; 35: 11188-93.

[18] Yu F, Zhang Y, Yu L, Cai W, Yuan L, Liu J, et al. All-solid-state direct carbon fuel cells with thin yttrium-stabilized-zirconia electrolyte supported on nickel and iron bimetal-based anodes. Int J Hydrogen Energy 2016; 41: 9048-58.

[19] Xu H, Chen B, Liu J, Ni M. Modeling of direct carbon solid oxide fuel cell for CO and electricity cogeneration. Appl Energy 2016; 178: 353-62.

[20] Lei L, Wang Y, Fang S, Ren C, Liu T, Chen F. Efficient syngas generation for electricity storage through carbon gasification assisted solid oxide co-electrolysis. Appl Energy 2016; 173: 52-8.

[21] Liu J, Barnett SA. Operation of anode-supported solid oxide fuel cells on methane and natural gas. Solid State Ionics 2003; 158: 11-6.

516 [22] Lin Y, Zhan Z, Barnett SA. Improving the stability of direct-methane solid oxide
517 fuel cells using anode barrier layers. J Power Sources 2006; 158: 1313-6.

518 [23] Murray EP, Tsai T, Barnett S. A direct-methane fuel cell with a ceria-based anode.
519 Nature 1999; 400: 649-51.

520 [24] Zhan Z, Barnett SA. An octane-fueled solid oxide fuel cell. Science 2005; 308:
521 844-7.

522 [25] Weber A, Ivers-Tiffée E. Materials and concepts for solid oxide fuel cells
523 (SOFCs) in stationary and mobile applications. J Power Sources 2004; 127:
524 273-83.

525 [26] Liso V, Cinti G, Nielsen MP, Desideri U. Solid oxide fuel cell performance
526 comparison fueled by methane, MeOH, EtOH and gasoline surrogate C8H18.
527 Appl Therm Eng 2016; 99: 1101-9.

528 [27] Qin H, Zhu Z, Liu Q, Jing Y, Raza R, Imran S, et al. Direct biofuel
529 low-temperature solid oxide fuel cells. Energ Environ Sci 2011; 4: 1273-6.

530 [28] Singh D, Hernández-Pacheco E, Hutton PN, Patel N, Mann MD. Carbon
531 deposition in an SOFC fueled by tar-laden biomass gas: a thermodynamic analysis.
532 J Power Sources 2005; 142: 194-9.

533 [29] Omosun A, Bauen A, Brandon N, Adjiman C, Hart D. Modelling system
534 efficiencies and costs of two biomass-fuelled SOFC systems. J Power Sources
535 2004; 131: 96-106.

536 [30] Seitarides T, Athanasiou C, Zabaniotou A. Modular biomass gasification-based
537 solid oxide fuel cells (SOFC) for sustainable development. Renew Sust Energy
538 Rev 2008; 12: 1251-76.

539 [31] Elleuch A, Boussetta A, Yu J, Halouani K, Li Y. Experimental investigation of
540 direct carbon fuel cell fueled by almond shell biochar: part I. Physico-chemical

541 characterization of the biochar fuel and cell performance examination. Int J
542 Hydrogen Energy 2013; 38: 16590-604.

543 [32] Liu M, Choi Y, Yang L, Blinn K, Qin W, Liu P, et al. Direct octane fuel cells: A
544 promising power for transportation. Nano Energy 2012; 1: 448-55.

545 [33] Jiang C, Ma J, Bonaccorso AD, Irvine JT. Demonstration of high power, direct
546 conversion of waste-derived carbon in a hybrid direct carbon fuel cell. Energ
547 Environ Sci 2012; 5: 6973-80.

548 [34] Lei L, Bai Y, Liu J. Ni-based anode-supported Al2O3-doped-Y2O3-stabilized
549 ZrO2 thin electrolyte solid oxide fuel cells with Y2O3-stabilized ZrO2 buffer layer.
550 J Power Sources 2014; 248: 1312-9.

551 [35] Cai W, Zhou Q, Xie Y, Liu J. A facile method of preparing Fe-loaded activated
552 carbon fuel for direct carbon solid oxide fuel cells. Fuel 2015; 159: 887-93.

553 [36] Wu C, Williams PT. Pyrolysis–gasification of plastics, mixed plastics and
554 real-world plastic waste with and without Ni–Mg–Al catalyst. Fuel 2010; 89:
555 3022-32.

556 [37] Xiao J, Xie Y, Liu J, Liu M. Deactivation of nickel-based anode in solid oxide
557 fuel cells operated on carbon-containing fuels. J Power Sources 2014; 268:
558 508-16.

559 [38] Yuan L, Li T, Saito K. Growth mechanism of carbon nanotubes in methane
560 diffusion flames. Carbon 2003; 41: 1889-96.

561 [39] De Jong KP, Geus JW. Carbon Nanofibers: Catalytic Synthesis and Applications.
562 Catal Rev 2000; 42: 481-510.

563 [40] Zhu X, Li Y, Lü Z. Continuous conversion of biomass wastes in a
564 La0.75Sr0.25Cr0.5Mn0.5O3–δ based carbon–air battery. Int J Hydrogen Energy
565 2016; 41: 5057-62.

566 [41] Zhang Y, Yu F, Wang X, Zhou Q, Liu J, Liu M. Direct operation of Ag-based
567 anode solid oxide fuel cells on propane. J Power Sources 2017; 366: 56-64.
568